ORIGINAL RESEARCH **Open access**

A Functional Safety-Oriented Framework for Perception System Design in Autonomous Mobile Machines

Hassan Ali[1*], Mariam Farooq[1], Usman Shah[2], Bilal Khan[3], Sana Malik[4]

Abstract

Ensuring safe and reliable environmental perception is vital to the operation of highly automated or fully autonomous agricultural machinery. Nevertheless, even with the growing need for robust perception systems, studies offering a broad, general method for designing and evaluating their functional safety and dependability remain scarce. This paper outlines the design and verification process for establishing a functionally safe and reliable perception system in a general framework. The relevant normative references — ISO 25119, ISO 21448, and ISO 18497 — concerning functional safety for highly automated mobile machines and vehicles are presented. The paper details the underlying concept and key factors involved in perception system design. A novel metric, “perception density,” is introduced as a standardized measure for assessing the spatial resolution of diverse perception sensors. Test scenarios were created to validate sensor performance under realistic working environments, covering target obstacles, expected visibility limitations, testing locations, and varying illumination settings. Results from the tests were examined and assessed against the established design criteria, with the perception sensors receiving a quasi-numerical rating through the defined evaluation process.

Keywords Evaluation, Highly automated agricultural machine, Perception system, Perception sensor, Safety of the intended functionality, Design considerations

*Correspondence:
Hassan Ali
hassan.ali@uaf.edu.pk
[1] Department of AI for Cotton Leaf Curl Virus Detection, Faculty of Agriculture, University of Agriculture Faisalabad, Faisalabad, Pakistan
[2] Department of Smart Canal Water Distribution Algorithms, Faculty of Agriculture, National University of Sciences and Technology, Islamabad, Pakistan
[3] Department of Machine Learning for Pest Outbreak Prediction, Faculty of Agriculture, University of Punjab, Lahore, Pakistan
[4] Department of Precision Herbicide Spraying, Faculty of Agriculture, University of Karachi, Karachi, Pakistan

Introduction

Agricultural automation has taken over some human tasks, bringing benefits such as improved product quality and reduced manufacturing costs [1]. Following the progress seen in autonomous vehicles, agricultural equipment incorporates advanced technologies and sensors and has handled specific operations automatically for many years. For example, multiple tractor manufacturers offer global navigation satellite system (GNSS) auto-steering options that manage tractor movement during portions of its working cycle [2]. Yet, the operator is still required to supervise activities to maintain safety. Achieving highly automated functions without any human involvement demands that machines collect and interpret surrounding data to prevent dangerous scenarios. Hence, deploying a perception system is critical, as it provides essential data for secure machine control and holds substantial promise for reducing hazards [3].

This is an open access article distributed under the terms of the Creative Commons Attribution-NonCommercial-ShareAlike 4.0 International License (CC BY-NC-SA 4.0), which permits non-commercial use, distribution, reproduction, and adaptation in any medium or format, provided that appropriate credit is given to the original author(s) and source, a link to the license is provided, and any changes made are indicated. Adapted material must be distributed under the same license.

© 2025 The Author(s). | Published by Agro Intelligence Research Press

Per ISO 18497, a highly automated agricultural machine (HAAM) requires a perception system that can identify, within expected operating situations, (1) objects lying in its travel path, (2) individuals coming near it, and (3) the machine's location in relation to recognized obstacles. Furthermore, the HAAM needs to establish the limits of the warning zone, where a clear alert — for instance, an audible or visual signal — activates to indicate the separation between the machine and the recognized object [3, 4]. Nonetheless, creating a highly capable, safe, and dependable perception system involves considerable difficulties. No single perception sensor performs flawlessly across every condition to encompass the full required detection area. Perception sensors inherently carry the risk of malfunction, incorrect readings, or delayed obstacle identification. In real-world use, sensor confidence can drop below the minimum acceptable level required for secure operation [3]. As a result, designing a functionally safe and reliable perception system must address not only technical capabilities but also operational and environmental factors that affect detection confidence [3, 5].

Lately, automation studies have incorporated perception systems across different autonomous platforms. For example, Christiansen [6] suggested a multi-sensor setup, TractorEYE, designed for secure driverless mowing, integrating LiDAR, a stereo camera, a thermal camera, a global positioning system (GPS), and an inertial measurement unit (IMU). LiDAR-enabled detection of objects extending above ground level and prevented impacts regardless of lighting conditions. The stereo camera was chosen for its ability to provide 3D depth alongside color details, aiding object detection and categorization under strong daylight. Thermal imaging succeeded at locating objects hidden from normal view, including humans or wildlife, though results varied greatly with object and ambient temperatures. The GPS and IMU provided precise details on the mower's orientation and location. Moorehead and colleagues created an autonomous platform for grass cutting and chemical application within citrus groves. This platform featured a perception setup to interpret the surroundings around the grove and detect barriers. A 2D LiDAR attached to a nodding motor enabled complete 3D environmental scanning. Depth data and visual inputs were merged to recognize and categorize barriers according to shape, surface patterns, and hues [7]. Blume and co-authors introduced an assistance tool for implementers that enhances usability, output standards, and protection.

A stereo camera fitted at the back of the tractor cabin ceiling captured 3D depth views of the rear area to identify and categorize implement placements [8]. Portugal and the team assembled a perception system with multiple sensors supporting driverless operation. A 2D LiDAR on a rotating mount measured object ranges and constructed 3D scene models. Stereo cameras captured detailed environmental features and performed visual odometry to track position. Real-time kinematic (RTK)-GPS, IMU, and movement data were integrated via an Extended Kalman Filter to refine location accuracy [9]. In January 2022, John Deere launched a fully autonomous tractor equipped with GPS and six stereo camera pairs, enabling 360° barrier detection and range measurement. Camera feeds were processed by a deep neural network on two NVIDIA Jetson GPUs, with pixel classification performed roughly every 100 ms to determine whether to continue or halt [10].

While substantial work exists on the creation of perception systems for HAAMs, generalized strategies for designing and evaluating safe and dependable perception remain underrepresented. The central aim of this paper is to deliver a broad methodology covering safety specifications, verification techniques, and relevant factors to achieve suitable safety levels in perception systems.

Our prior research [5] introduced an organized method for judging sensor appropriateness in specific applications. This method accounts for both engineering specifications and real-world operational factors while setting assessment standards. It functions as a practical resource for engineers choosing appropriate sensors or sensor groups during safe perception system development. That said, the earlier work lacked guidance on executing actual field evaluations of sensor effectiveness. Such sensor-by-sensor assessment forms a core part of the overall procedure.

This paper provides foundational principles for creating and verifying a functionally safe and reliable perception system. The assessment approach detailed in the previous paper [5] was used to evaluate various perception sensors in authentic operational settings. The defined goals include: (1) establishing design factors for a functionally safe and reliable perception system; (2) performing on-site experiments to review perception sensor capabilities for barrier

© 2025 The Author(s). | Published by Agro Intelligence Research Press

detection in realistic scenarios; and (3) examining and judging sensor suitability while incorporating technical output, reliability of detection, and operational realities.

The paper follows this sequence: Normative references related to safety design for highly automated mobile machines and vehicles come first. Next, the core idea and design factors for perception systems are explained. A testing approach using a sensor evaluation platform then appears. Lastly, test outcomes are analyzed and appraised according to the evaluation procedure.

Related Literature

This section addresses fundamental concepts of perception systems and sensors, along with three safety standards (ISO 25119, ISO 21448, and ISO 18497) essential to constructing a safe and reliable perception system.

Safety standards

ISO 25119 represents the main functional safety guideline for agricultural equipment. It concentrates on identifying and resolving electric/electronic (E/E) system malfunctions that might compromise safety objectives [11]. In highly automated setups, safety extends beyond E/E defects to include additional hazards, such as operator misuse, sensor or system capability constraints, and unexpected environmental shifts [12]. ISO 21448 addresses hazards that arise independently of system malfunctions [12]. Rather than E/E faults, it addresses scenarios in which the planned design proves inadequate or unsuitable for ensuring user safety when no faults exist **(Figure 1)**.



Figure 1. Risk scope of ISO 25119 and ISO 21448. Faults of E/E safety-related systems are covered by ISO 25119. Insufficiencies in the specification of intended functionality at the machine level and in the implementation of E/E systems are covered by ISO 21448 [11, 12].

ISO 21448 revolves around the term “SOTIF”, meaning Safety of the Intended Functionality. This method applies a repeated development cycle focused on confirming and approving system behavior at a tolerable risk level. It presumes a defined safe operation zone alongside an uncertain zone that may pose danger, as illustrated in **Figure 2**. The white area indicates safe, known conditions. SOTIF’s goal is to review areas 2 and 3, reduce hazards associated with both familiar and unfamiliar actions, and demonstrate that residual risks remain tolerable. Hardware or conceptual/software faults must not produce dangerous outcomes across varied environmental conditions. Identification and reduction of such risks occur via experiments, modeling, and statistical review of perception sensors and systems. ISO 21448 excludes the

© 2025 The Author(s). | Published by Agro Intelligence Research Press

assessment of hardware failure faults and instead targets risks stemming from design concepts that operate correctly without faults. The current research examined and rated potential perception sensor risks under SOTIF conditions using real-world testing.



Figure 2. Definition for possible function and system behaviour [12]. The SOTIF approach aims to evaluate and address potential hazards arising from both known and unknown scenarios in areas 2 and 3. By minimizing these potential dangers, the approach seeks to provide evidence that any remaining hazards are acceptable.

Perception system

According to ISO 18497, a highly automated agricultural machine (HAAM) must include a perception system capable of identifying, under expected operating conditions, objects lying in the HAAM's path, individuals coming near the HAAM, and obstacles in relation to the HAAM's position. Additionally, it must define the limits of the warning zone, where a clear alert is issued to show the distance between the machine and the detected object [3]. A perception system depends greatly on perception sensors that collect data on the HAAM's environment along with algorithms designed for detecting, localizing, and classifying relevant features **(Figure 3)**. Therefore, an environmental perception system holds strong potential to minimize safety hazards in machine operation through automated control that does not require any operator involvement.

© 2025 The Author(s). | Published by Agro Intelligence Research Press

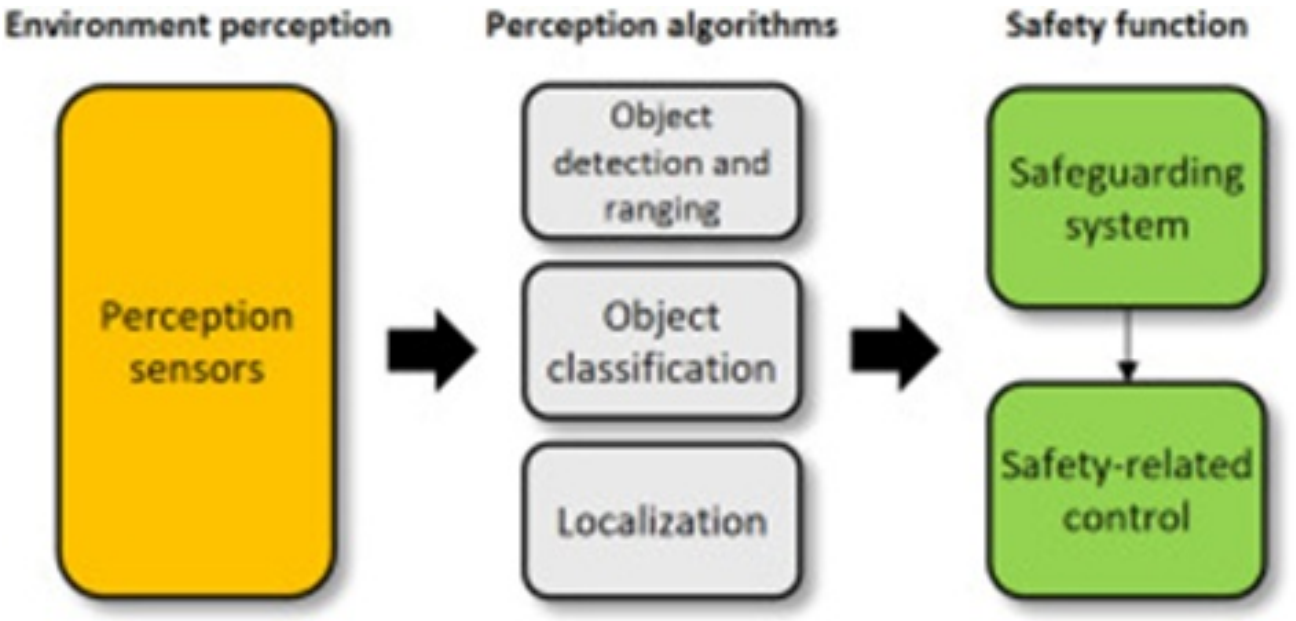

Figure 3. Configuration of perception system. Employing a perception system that relies on sensors and algorithms to identify key features in a machine's environment supports safer operation without operator input and reduces safety risks.

State-of-the-art perception sensors

This section presents the most representative perception sensors that constitute a perception system, as follows [6-10, 13]: RGB camera, stereo camera, thermal camera, continuous wave-time-of-flight (CW-ToF) camera, LiDAR, and frequency-modulated continuous wave (FMCW) Radar.

RGB cameras are imaging devices that gather visible light and convert it into electrical signals, which are then processed to create images and video sequences. The majority of RGB cameras use either a charge-coupled device (CCD) or a complementary metal-oxide-semiconductor (CMOS) sensor. These devices are built to record light in red, green, and blue wavelengths to ensure precise colour reproduction and operate within the 400 nm to 700 nm wavelength range, matching the spectrum visible to the human eye. Contemporary security and surveillance cameras offer multiple lens options and deliver images in high-definition (HD) or higher resolution. By incorporating machine learning and deep learning techniques, RGB cameras can now identify physical forms and approximate scene depth from a single image [14].

RGB cameras can be used for object detection in the surroundings using machine learning approaches. For example, an RGB camera may detect items around a tractor by capturing a scene image, then processing it with computer vision algorithms to extract image features. These features are then applied to recognize and locate objects in images [15, 16]. RGB cameras can further identify significant elements in the scene, including crops and drivable terrain, while also recognizing dividing lines between crops and accessible ground [17].

Thermal cameras generate images according to the temperature of objects rather than their visual characteristics. They detect thermal radiation emitted by living creatures in moderate and cold climates and function effectively in total darkness without requiring an additional light source. Microbolometer detectors are frequently employed in thermal cameras that operate in the Long-wave infrared (LWIR, 7.5–14 μm) spectrum and do not require cooling [18].

Thermal cameras are applicable not only for detecting people but also for spotting wildlife in fields, even under dim or zero lighting, which supports environmentally conscious farming practices [6, 19, 20].

© 2025 The Author(s). | Published by Agro Intelligence Research Press

Stereo cameras emulate human binocular vision. They capture two images simultaneously with cameras positioned apart, where the value of each pixel depends on the distance from the sensor to the corresponding scene point. Stereo cameras deliver both intensity images and associated depth maps; however, their effective range is usually limited, as depth uncertainty scales with the square of the distance. A frequent issue is that surfaces lacking texture cannot be properly matched, leading to gaps in the resulting 3D data [21].

Stereo cameras can be utilized not only for detecting and positioning objects around a vehicle but also for recognizing fixed obstacles, thereby enabling the creation of 3D maps [6, 22]. Stereo cameras can also be installed on agricultural tractors to detect crop rows by measuring height differences between crops and the soil. This data can subsequently support automatic tractor steering to remain inside the crop rows and prevent crop damage [23].

CW-ToF cameras determine distance by emitting a modulated light beam, such as a laser beam, toward an object and using a sensor tuned to the near-infrared range around 850 nm to record the returning light. Distance values are acquired using a 2D pixel array that requires no mechanical components. ToF sensors use a CMOS sensor to convert optical signals into electrical signals. Accuracy is constrained by the strength of the transmitted IR signal, which is typically weak relative to ambient daylight and interferes with the reflected signal. Moreover, both depth precision and frame rate are limited by the ToF camera's integration time. Extended integration time generally improves depth measurement accuracy, yet recording moving objects at a constant frame rate restricts this time, thereby decreasing accuracy [24].

CW-ToF cameras can generate crop-field maps that support accurate positioning and self-directed navigation for the tractor [25]. CW-ToF cameras can further assist in detecting and harvesting fruits by assessing fruit depth and colour. Such details enable automation of the fruit collection procedure [26].

LiDARs are optical remote sensing methods that measure the distance to or additional attributes of a target using light emission. This approach relies on the time-of-flight concept, which calculates the time required for a laser pulse to travel a specific distance through a medium. Lasers operating between 600 nm and 1000 nm are typically selected for LiDAR systems because of their affordability, although eye-safety regulations restrict their maximum power output. As an option, 1550 nm lasers offer higher safe power levels and extended detection ranges than shorter wavelengths. LiDAR produces range information about nearby points and constructs a point cloud, where each point includes its 3D coordinates and the intensity of its reflected signal. Nevertheless, challenging weather conditions, such as heavy rain, dust, or fog, can impair LiDAR performance. Raindrops may bounce the beam back, causing the system to register them as objects, and can also absorb portions of the emitted light, thereby shortening the operational range [27].

LiDARs can facilitate autonomous tractor guidance by providing live environmental information, ensuring secure, clear pathways even in poor-visibility scenarios such as nighttime [6]. LiDARs can also be combined to enable automatic weed identification and elimination, enabling targeted, precise herbicide application, which in turn reduces chemical use and ecological impacts [28, 29].

FMCW radars, also known as radio detection and ranging, transmit radio waves across the 3 MHz to 110 GHz spectrum that bounce off objects to calculate their distance, direction, and velocity. The separation between the transmitter and the object is found by measuring the round-trip time of the signal and its echo. However, the radar supplies no shape details. FMCW Radars perform well at recognizing large, highly reflective targets, but their performance declines with smaller or less reflective targets, such as people. Furthermore, radar signals penetrate effectively, making them suitable for object detection in difficult conditions, including fog, rain, wind, darkness, and intense sunlight. Still, FMCW Radars generally offer lower resolution than camera technologies and can have difficulty separating objects with similar traits. The transmitted signal may also generate false detections through multiple reflections [30].

FMCW Radars can support obstacle recognition and crash prevention, helping avoid mishaps and damage to machinery, particularly under reduced visibility [31]. FMCW Radars can additionally determine canopy height, permitting vegetation assessment during active agricultural tasks performed by machines or attached tools [32].

© 2025 The Author(s). | Published by Agro Intelligence Research Press

Design Considerations

The initial distribution of functional safety needs into the system architecture is outlined in the technical safety concept via technical safety requirements. Still, notable obstacles exist in delivering functionally safe and dependable perception, due to the risks associated with the planned functionality and its implementation [33]. Environmental perception arises from merging information from one or more perception sensors, followed by processing and evaluation through perception algorithms. Nevertheless, these sensors or algorithms might underperform in harsh or unexpected scenarios due to incomplete specifications or limited capabilities, leading to unsafe actions even without system faults. Perception sensors frequently miss obstacles or issue false alarms due to external factors, leading to dangerous outcomes. Thus, identifying potential hazards early, before product development, is vital [5].

Building a functional, safe, and dependable system means addressing not only technical specifications but also operational and external factors that affect each sensor's effectiveness [3, 11, 12]. This work presents three main design considerations for creating a perception system that meets safety, reliability, and practical-use requirements in the concept stage **(Figure 4)**: technical performance, detection reliability, and practical considerations.



Figure 4. Three aspects of design considerations for designing a functional, safe, and reliable perception system.

Technical performance measures how successfully a system meets its technical specifications or targets. Detection reliability is a measure of how consistently a system executes its planned role under actual conditions. Practical considerations serve as a guide to additional elements requiring attention when applying a system within machines.

The design considerations provide core guidance for selecting suitable sensors or sensor configurations that meet the requirements for safety, reliability, and application. Thorough coverage of technical performance, detection reliability, and practical considerations appears in Sections 3.1, 3.2, and 3.3, respectively.

© 2025 The Author(s). | Published by Agro Intelligence Research Press

Technical performance

Technical performance measures how successfully a system meets its technical specifications or targets. This section reviews current criteria and introduces the new criterion, “perception density” (see Section 3.1.2), needed for evaluating technical performance.

Existing criteria

Here is a list of key existing criteria for technical performance focused on the technical execution of a perception system:

• Perception range stands as a vital criterion for halting or dodging movement in reaction to an obstacle entering the hazard zone near a HAAM. It supports obstacle detection and stopping before contact, and the HAAM’s braking ability should be considered when setting the minimum perception range requirement [34].

• Range accuracy forms a major factor when gauging ranging precision in typical working conditions. Accuracy needs can stem from the necessary or projected precision of the targeted perception functions [35]. For example, automated vehicles need localization accuracy of less than 0.1 m and a confidence level of over 95% to reach SAE J3016TM level 4. The European Global Navigation Satellite Systems Agency (GSA) established accuracy standards for safety-critical automated driving at below 0.2 m precision with 99.9% availability [36].

• Refresh rate emerges as another essential factor, closely linked to perception-reaction time (PRT), described as the duration from initial detection to the actual response. Lowering the PRT reduces the HAAM’s stopping distance, especially at higher operating speeds [37].

• Field of view (FOV) and resolution establish the extent of environmental detail captured by a perception system, critical for secure operations [38]. IEC 62676 defines five levels of image detail, expressed in pixels per meter and referred to as pixel density (PPM). These five levels of image detail serve as a benchmark for assessing the potential image detail a camera can record at a chosen target distance [39]. Based on the image processing purpose, the required pixel density (RPPM) can be set; see **Table 1**.

Table 1. An example of five levels of image detail for a camera based on IEC 62676 [39].

Application purpose		Explanation	RPPM [pixels/m]
Monitoring		Allows operators to observe the movement, direction, and speed of individuals over a broad area, provided their presence is already known.	12.5
Detection		Enables operators to clearly and consistently verify whether a target, such as a person or vehicle, is present.	25
Observation		Permits viewing of distinguishing features, such as clothing details, while still maintaining awareness of activities occurring around the event.	62.5
Recognition		Allows operators to determine with high confidence whether an observed individual matches a previously seen individual.	125
Identification		Supports confirming the identity of an individual beyond a reasonable doubt.	250

Yet, the level of detail for a target under detection depends not only on sensor resolution and FOV, but also on the target’s distance (d). As shown in **Figure 5**, objects positioned closer to the target display higher PPM values. Greater PPM enables perception sensors to resolve tinier details. Thus, the required pixel density (RPPM) results from the combination of sensor resolution and FOV, along with the geometric link to the target object.

© 2025 The Author(s). | Published by Agro Intelligence Research Press

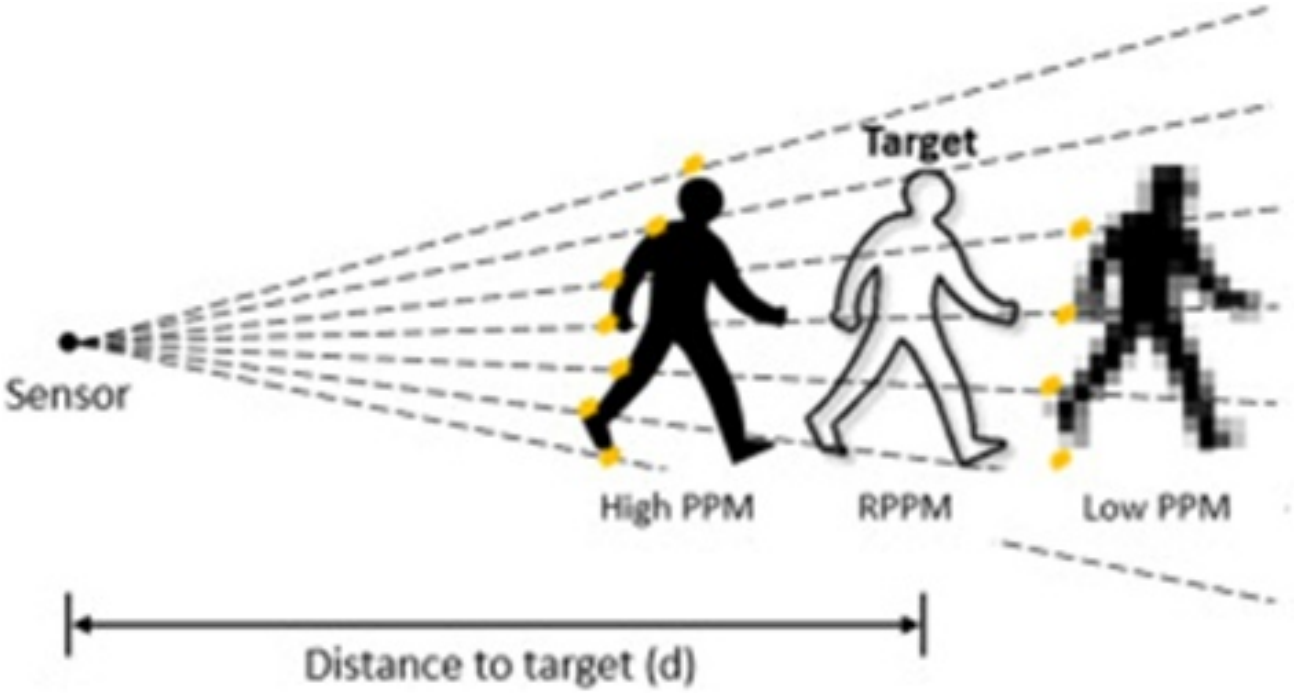

Figure 5. Conceptual image of “pixel density”.

Perception density

Although pixel density works well for setting the detail-level requirements for target detection, it is less effective for contrasting target detail levels across different sensors. Hence, we propose a new criterion, perception density (PD). This supports defining the necessary resolution and FOV for sensors in a perception system and allows uniform comparison of spatial resolution among varied perception sensors like cameras, LiDARs, and Radars **(Figure 6)**. Perception density equals the count of data points (unit: point(s)) produced by the sensor inside a specified FOV [5]. It delivers a wider approach to expressing spatial resolution density for both pixels and point clouds.

© 2025 The Author(s). | Published by Agro Intelligence Research Press

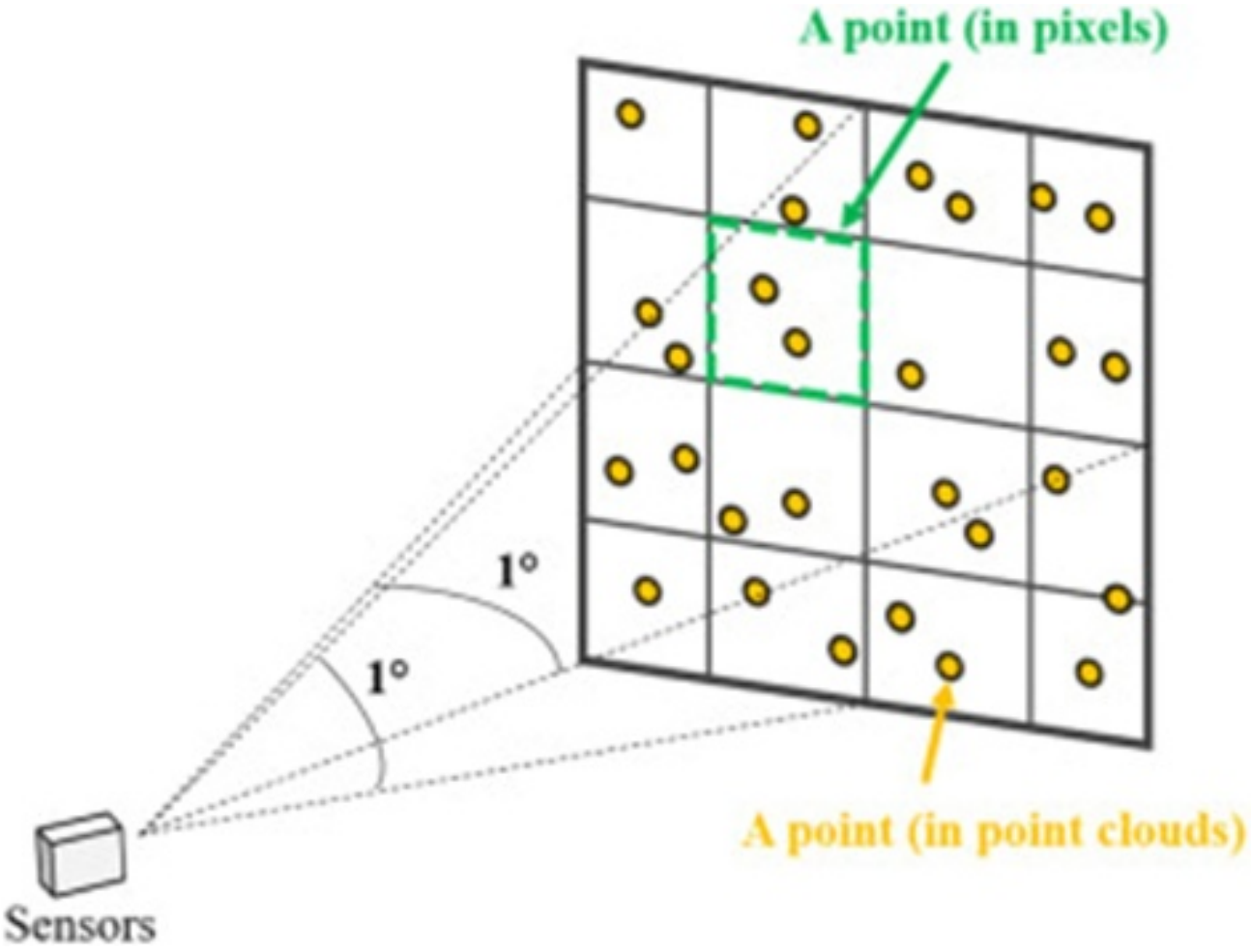

Figure 6. Conceptual image of criterion “perception density”. The unit “Point(s)” includes both pixels and point clouds generated by sensors such as cameras and LiDAR.

One-dimensional perception density (PDH or V) is calculated by dividing the horizontal (subscript “H”) or vertical (subscript “V”) sensor resolution by the corresponding horizontal or vertical field of view (FOVH or V). The square root of two-dimensional perception density (PDHV) equals the product of the two one-dimensional perception densities (PDH and PDV):

$$PD_{H\ or\ V} = \frac{\sum Points_{H\ or\ V}}{FOV_{H\ or\ V}} \quad (1)$$

$$PD_{HV} = \sqrt{PD_H \times PD_V} \quad (2)$$

Where:

• PDH or V: the one-dimensional perception density [points/°]

• PDHV: the square root of two-dimensional perception density [points/°]

© 2025 The Author(s). | Published by Agro Intelligence Research Press

• ∑PointsH or V: the number of horizontal or vertical points on a target [points]

• FOVH or V: the horizontal or vertical field of view [°]

The five levels of pixel density in IEC 62676 served as a reference for setting the detail level of an object detected at a given target distance. The required perception density (RPD), used to select appropriate perception sensors for object detection and classification at the target distance, is calculated from the required pixel density (RPPM) corresponding to a 1° FOV at that distance.

$$RPD_{H\ or\ V@d} = k\ \times d \times RPPM_{H\ or\ V} \quad (3)$$

$$RPD_{HV@d} = \sqrt{RPD_{H@d}\ \times\ RPD_{V@d}} \quad (4)$$

Where:

• RPPM H or V: required PPM [pixels/m]

• RPD H or V@d: required PDH or V for a target at the distance (d) [points /°]

• RPD HV@d: required PDHV for a target at the distance (d) [points /°]

• k: conversion coefficient value, k=2 tan (0.5°)

• d: distance between sensor and target [m]

Table 2 shows the results of RPDs based on the example RPPMs defined in IEC 62676. The detail level of a detected target (RPPMs) may vary based on use-case needs. Horizontal and vertical RPPM values do not have to match.

Table 2. The results of required perception densities (RPDs) based on required pixel densities (RPPMs). The RPDs were calculated based on a target at 8 m distance because a test platform was placed 8 m away from the obstacles.

Degrees of pixelization	$RPD_{HV@}$8 m [points/°]	$RPD_{H\ or\ V@}$8 m [points/°]	$RPPM_{H\ or\ V}$ [ppm]
Monitoring	*1.7*	*1.7*	*12.5*
Detection	*3.5*	*3.5*	*25*
Observation	*8.7*	*8.7*	*62.5*
Recognition	*17.5*	*17.5*	*125*
Identification	*34.9*	*34.9*	*250*

The chief benefit of adding “PD” is its ability to broaden comparisons beyond cameras alone to include additional perception sensors, such as LiDAR. Besides that, PPMs acting as requirement guides can be translated into perception density using geometric connections.

© 2025 The Author(s). | Published by Agro Intelligence Research Press

Detection reliability

"Detection reliability" is a measure of the consistency with which a system performs its designated role under actual operating conditions. **Figure 7** displays the grouping of possible malfunctions in a perception system, along with the risk factors that influence the detection reliability of perception sensors: environmental, obstacle-related, and machine-related parameters. Environmental parameters include multiple environmental pressures, such as sunlight, darkness, and various forms of atmospheric precipitation, as well as weather states. Obstacle-related parameters concern the characteristics of objects requiring identification, such as reflectance properties, object sizes, and object movement velocity. Machine-related parameters encompass hardware and software matters such as vibration, CPU load, part-specific problems, software faults, sensor misalignment, and increased operating speed. These risk factors can trigger improper operation in perception sensors, thereby reducing their confidence levels. To reduce or eliminate residual risks, every malfunction should be identified through perception sensor testing, while the perception system's performance should be confirmed in accordance with ISO 18497 [3].

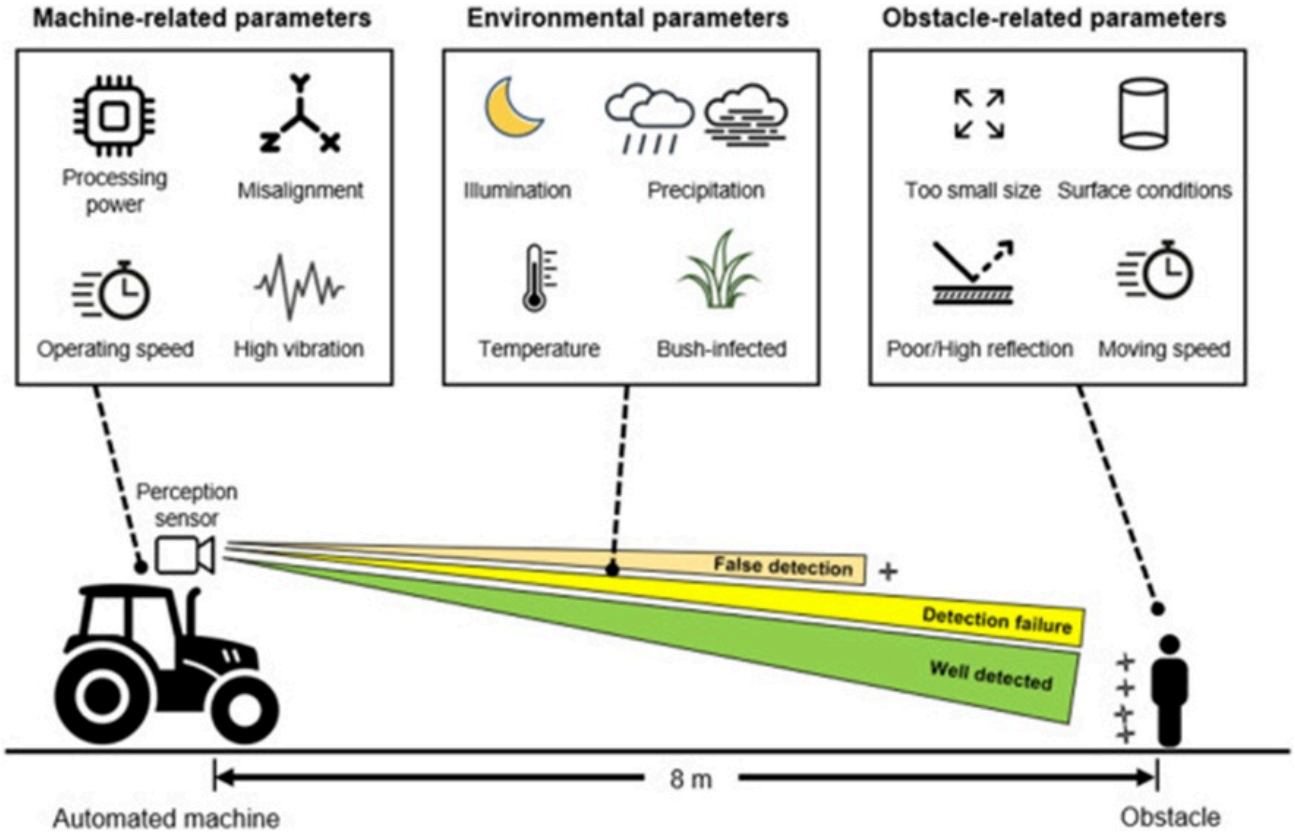

Figure 7. Possible perception failures and their causes [3].

Practical considerations

"Practical considerations" represent a measure of extra aspects linked to applying a system in machines. Such aspects could cover the items presented in **Table 3**.

Table 3. A list of practical considerations for the design of highly automated machines and vehicles [33].

Category	Reworded considerations
Practical considerations	General operational considerations

© 2025 The Author(s). | Published by Agro Intelligence Research Press

Technical/physical requirements	Active or passive operational response
	Connectivity interfaces
	Bandwidth requirements
	Processing/computational demand
	Data compression capability
	Maximum cable distance
	Power transmission through cable
	Energy consumption
	Computational processing cost
	Calibration needs
	Diagnostic capabilities
	Performance verification requirements
Environment and stress	IP-rated enclosure protection, resistance to shock and vibration
	Electrostatic discharge (ESD) protection
	Susceptibility to interference
	Operating temperature range
Legal requirements	Compliance with safety standards, regulations, and statutory requirements
Others	Overall cost
	Physical size/dimensions
	Weight specifications
	Secure mounting requirements
	Reliability during operation
	Plausibility verification
	Cooling mechanism requirements
	Maintenance, servicing, and cleaning needs
	Scalability potential
	Real-time operational capability

Evaluation

This section presents a test procedure to assess how perception sensors perform using a test sensor platform. The measurement outcomes will be reviewed for each scenario.

This section outlines a sample test approach to confirm and assess the performance demands placed on a perception system or its sensors. A sample use-case appears here within the setting of “autonomous grass mower with obstacle detection” [5]. The autonomous grass mower has to satisfy the listed requirements:

© 2025 The Author(s). | Published by Agro Intelligence Research Press

• Operate at up to 33 km/h (with a stopping distance of at least 8 m).

• Perception-reaction time (PRT) of 100 ms.

• Detect and range objects within 10 cm accuracy.

• Perform GNSS-based localization.

• Classify obstacles above the observation level in IEC 62676.

• Safely control the mower.

The system must function under both bright and low-light conditions (above 2 lux) and in moderate rain (above 1.5 l/m2). The chief source of stress comes from physical hazards, such as trees and people. Limitations of the system include an inability to handle obstacles that are too small or too negative, as well as harsh weather conditions such as heavy rain, snow, and fog.

Test method

Table 4 presents various test scenarios designed to handle realistic operational situations, accounting for targeted detection obstacles, anticipated visibility reductions, test locations, and varying lighting conditions. Scenarios 1 and 2 aimed to examine the performance of perception sensors under standard conditions. The purpose of test scenarios 3 and 4 was to assess the influence of typical operating conditions that lead to obstacle obscuration on detection confidence. Test scenario 5 aimed to explore how passive technologies perform in low-light and completely dark settings.

Table 4. An overview of test scenarios. The environmental conditions were measured on-site using a test sensor platform.

Test cases	Surface conditions	Environmental conditions (Lighting/Temperature/Relative humidity)	Key characteristics	Scenario illustration	Description image
Standard conditions	1	Grass surface	31,000 Lux / 9 °C / 42%	Conducted on a grassy area	
	2	Asphalt tile surface	100 Lux / 0.6 °C / 67%	Performed inside a parking structure	
Predictable obstruction	3	Dense/tall grass	7300 Lux / 13 °C / 59%	An individual concealed within tall grass	
	4	Asphalt roadway	2800 Lux / 12 °C / 61%	Moderate rainfall at 1.5 L/m²	
Reduced visibility	5.1	Asphalt roadway	2 Lux / 20 °C / 65%	Dim-light environment	
	5.2	Asphalt roadway	1 Lux / 11 °C / 72%	Near-darkness conditions	

© 2025 The Author(s). | Published by Agro Intelligence Research Press

Five test obstacles were selected based on obstacle-related features that affect detection confidence (as indicated in **Table 5**). Each obstacle has its own distinct shape, material properties, and surface state. The ISO barrel, defined per ISO 18497, corresponds to a seated human being filled with water to imitate human body makeup and is made of olive-green plastic [3]. Additional test barriers comprised a person, green and black waste containers, plus a road sign.

Table 5. Overview of test obstacles.

Obstacle type used in testing	Material composition	Surface properties	Supplementary details	Obstacle image
ISO barrel	Plastic	Olive-green appearance; curved, non-glossy surface	Specified according to ISO 18497; designed to simulate a seated person; filled with water	
Human subject	Human body	Everyday clothing; reflective safety vest		
Green waste bin	Plastic	Green-colored finish; smooth, texture-free surface		
Black waste bin	Plastic	Black-colored finish; smooth, texture-free surface		
Traffic sign	Metal	Flat metallic surface	Arrow-logo marking; reflectivity rating: RA2	

Test platform

Figure 8 illustrates a test platform built from four core elements: perception sensors, a control unit, a portable battery, and a laptop PC.

© 2025 The Author(s). | Published by Agro Intelligence Research Press

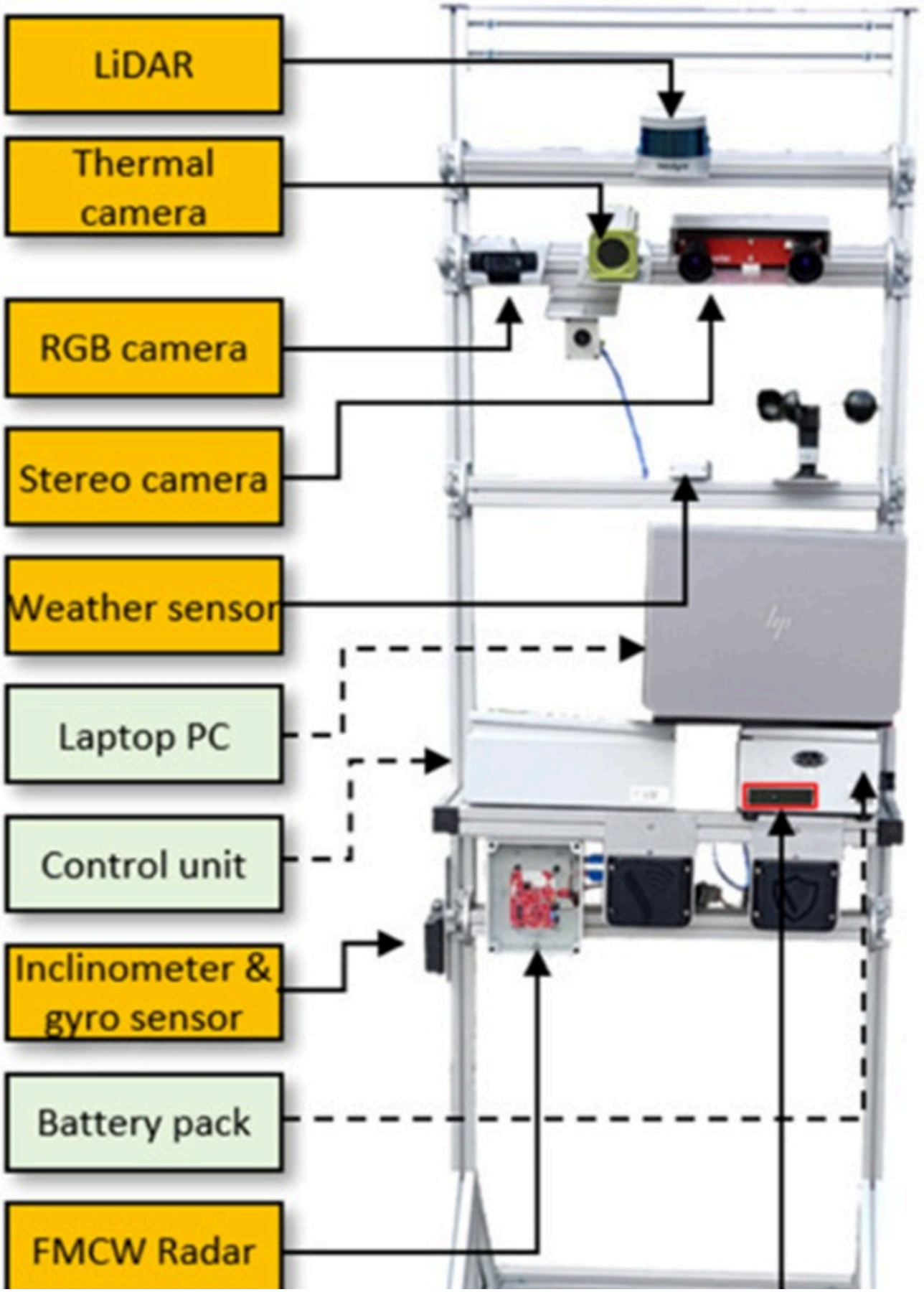

© 2025 The Author(s). | Published by Agro Intelligence Research Press



Table 6. Specification of the perception sensors mounted on the test platform, as shown in **Figure 8**.

Sensor category	Manufacturer/Model	Operating wavelength	Viewing angle (Horizontal × Vertical)	Resolution	Sensor data output
RGB imaging camera	Logitech (C920)	400–700 nm	78° × 49°	1920 × 1080	• Color imagery
Thermal imaging camera	FLIR (Boson 640)	7500–13,500 nm	50° × 41°	640 × 512	• Thermal imaging output
Stereo vision camera	Nerian (Karmin 3D Stereo camera)	400–700 nm	61.6° × 48.1°	1600 × 1200	• Grayscale image• Disparity mapping (0.8 to 15 m)• Point cloud generation
ToF camera (Continuous Wave type)	PMD (Pico flexx)	850 nm	62° × 45°	224 × 171	• Depth mapping (0.1 to 4 m)• Intensity image
Rotational LiDAR sensor	Velodyne (VLP-16)	905 nm	360° × 30°	Angular resolution (up to 0.1° × 2°)	• Point cloud data (maximum range: 100 m)• Angular resolution (up to 0.1° × 2°)
FMCW radar sensor	Texas Instrument (TI-IWR1642)	3.7–3.9 mm	120° × 30°	Supports up to 250 points	• Point cloud output (range up to 80 m)• Velocity measurement (maximum 5.25 m/s)• Azimuth angle (up to 160°)• SNR (signal-to-noise ratio)
Environmental monitoring sensor	BlueDot (Advanced weather station)	—	—	—	• Illumination measurement (0 to 65,535 lux)• Temperature sensing (−40 to 85 °C)• Humidity detection (0 to 100%)
Inclinometer and gyroscope	Sensor Technik Wiedemann (NGS2)	—	—	—	• Inclination range: ±180°• Gyroscope range: ±50°/s

© 2025 The Author(s). | Published by Agro Intelligence Research Press

sensor					

Test obstacles were placed at an adequate distance from the sensor platform, allowing the image to occupy approximately one quarter of the monitor's vertical height [33]. The test platform was placed 8 m from the obstacles, calculated from the braking distance for a vehicle moving at its maximum speed of 33 km/h [34]. The ToF camera was used exclusively at a 4 m distance from the obstacles due to its limited field of view.

Measurement analysis and discussion

This section presents the measurement outcomes, along with discussions related to the five scenarios listed in **Table 4**. The test platform was used to measure the test obstacles in each scenario. For scenarios 1, 4, and 5, the test obstacles included an ISO barrel, a person, green and black waste containers, and a road sign, in that order. For scenarios 2 and 3, the test obstacles involved the person and the ISO barrel in that order.

On grass and in parking lot environments (test scenario 1)

Figure 9, together with **Figure 10**, presents results from various perception sensors in a field covered with low grass on a sunny day and in a parking garage, respectively.

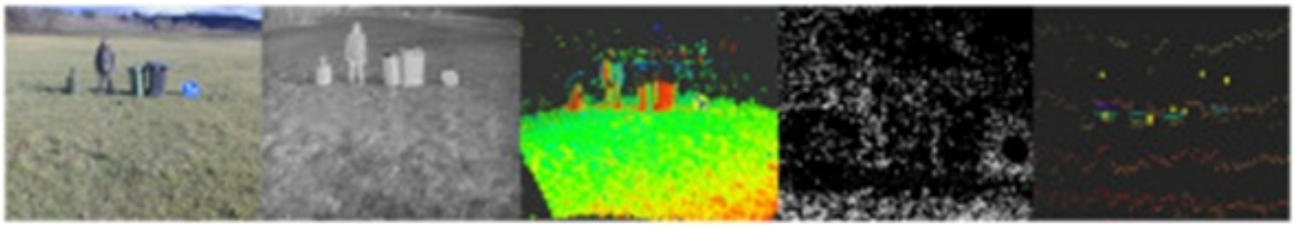

Figure 9. Test results measured by an RGB camera (leftmost), a thermal camera (second leftmost), a stereo camera (middle), a ToF camera (second rightmost), and both a LiDAR (rightmost, circle points) and an FMCW Radar (rightmost, yellow squares) on grass.

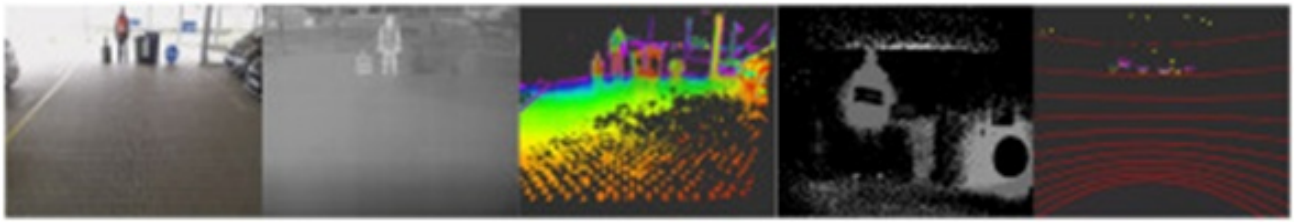

Figure 10. Test results measured by an RGB camera (leftmost), a thermal camera (second leftmost), a stereo camera (middle), a ToF camera (second rightmost), and both a LiDAR (rightmost, circle points) and an FMCW Radar (rightmost, yellow squares) in a parking garage.

[RGB camera] Owing to contrasts in colour plus brightness compared against the background, every test obstacle proved identifiable across both test scenarios, evident inside the RGB images from **Figure 9** (leftmost) and **Figure 10** (leftmost). Especially, although the ISO barrel on the grass possessed a colour close to that of the grass, it remained identifiable through the shadow it cast.

[Thermal camera] Across the thermal images (**Figure 9**, second from the left, and **Figure 10**, second from the left), separation of all grass-placed obstacles from the background succeeded. Nevertheless, inside the parking garage, the waste containers and the road sign exhibited weak contrast against the background, as their temperatures closely matched those of the adjacent surroundings, which lacked direct sunlight. On the contrary, the person and the ISO barrel produced marked thermal contrast, as the heat capacity of body water remained high, thereby hindering rapid heat transfer to the air. Identification of the arrow symbol on the road sign was not possible with the thermal camera, as

© 2025 The Author(s). | Published by Agro Intelligence Research Press

thermal imaging relies on temperature differences for obstacle recognition, which limits its capability when surface temperatures across obstacles remain uniform, as with printed text or images.

[Stereo camera] Outcomes from the stereo camera point cloud demonstrated that dense 3D point clouds permitted measurement of morphological characteristics belonging to the obstacles and the ground inside both scenarios, noticeable in **Figure 9** (middle) and **Figure 10** (middle). Nonetheless, pixels in texture-free zones or areas with repeated patterns failed to match, leaving some portions of the waste containers and parking garage ground tiles without measurement. Recognition of the arrow symbol on the road sign was enabled by the intensity values associated with each point, which provide valuable characteristics for object recognition, including textures, patterns, and image contrast. Even so, noisy depth calculations and outliers emerged due to image defects, triangulation inaccuracies, depth quantization, and matching uncertainties.

[ToF camera] Depth images produced by the ToF camera (**Figure 9**, second from the right, and **Figure 10**, second from the right) indicated that distinguishing all grass-placed obstacles from the background proved challenging. Influences, including ambient light noise, photon shot noise, phase wrapping, multipath interference, and related issues, likely contributed to flawed depth readings. Inside the parking garage, a large number of unreliable detections occurred. Due to surface shapes, portions of the emitted light were not reflected toward the ToF camera, resulting in unclear detection of the ISO barrel and the left side of the green waste container. Detection failed for the person's black trousers and the black garbage container due to black's strong light-absorbing properties. Measurement was not performed for the road sign or the reflective vest stripes because highly reflective items returned excessive light that saturated the sensor pixels. Light scattered in the space between the lens fixed to the sensor and the pixels led to corrupted distance measurements.

[LiDAR and FMCW radar] **Figure 9** (rightmost), along with **Figure 10** (rightmost), exhibit outcomes acquired through LiDAR and FMCW Radar. Accurate and consistent measurements covered the test obstacles and the ground across both scenarios, as evident from the LiDAR results shown in **Figure 9** (rightmost). Neither the curved surface on the ISO barrel nor the highly reflective surfaces on the road sign and reflective vest affected range performance. Still, the level of detail remained limited due to the small object size and the longer distance to the LiDAR.

Conversely, outcomes from FMCW Radar (**Figure 10**, rightmost) reveal that detection succeeded for only a small number of obstacles across ranges and azimuth angles. Both Radar range accuracy and repeatability remained inferior to LiDAR, while separating nearby obstacles proved difficult due to the limited angular resolution. Furthermore, multipath propagation associated with radar echoes produced several false signals behind obstacles, thereby generating considerable measurement uncertainty that could diminish ranging precision and overall reliability within the perception system.

Tall grass environment (test scenario 2)

Figure 11 illustrates the outcomes obtained from multiple perception sensors placed in front of tall grass concealing a hidden person.

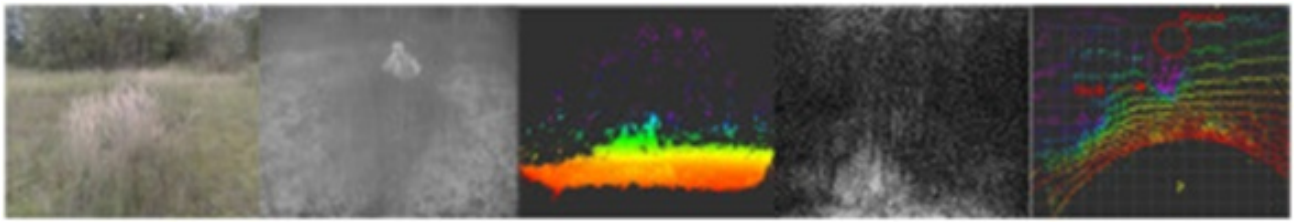

Figure 11. Test results measured by an RGB camera (leftmost), a thermal camera (second leftmost), a stereo camera (middle), a ToF camera (second rightmost), and both a LiDAR (rightmost, circle points) and an FMCW Radar (rightmost, yellow squares) in front of tall grass.

© 2025 The Author(s). | Published by Agro Intelligence Research Press

The RGB camera (leftmost in **Figure 11**) proved incapable of separating the person from surrounding elements, as visible light was blocked by the dense, tall grass.

By comparison, the thermal camera (second position from left in **Figure 11**) achieved greater penetration depth into the vegetation, rendering it useful for viewing through dense grass clusters.

The stereo camera, ToF camera, LiDAR, and FMCW Radar (positions from middle through rightmost in **Figure 11**) were unsuccessful in locating the person concealed within the thick vegetation mass and registered detections exclusively outside the vegetation area.

Moderate rain condition (test scenario 3)

Figure 12 shows the outcomes generated by various perception sensor types on a day with moderate rainfall, roughly 1.5 L/m2. Usage was restricted to the ISO barrel as the sole obstacle to eliminate cross-interference, since laser or radar returns from nearby items risked producing false readings and complicating proper examination of rainfall influences.

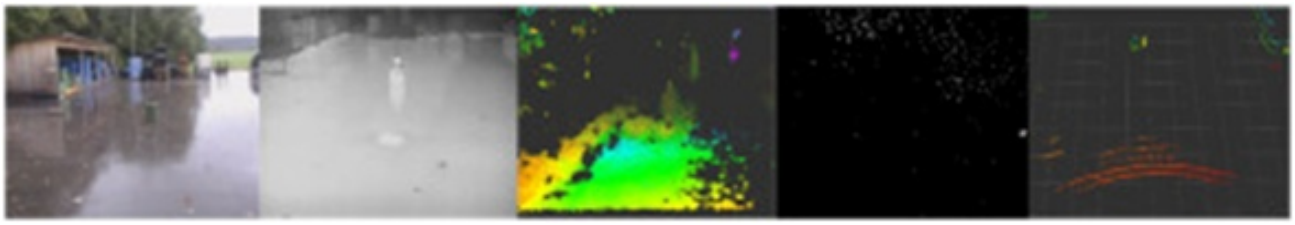

Figure 12. Test results measured by an RGB camera (leftmost), a thermal camera (second leftmost), a stereo camera (middle), a ToF camera (second rightmost), and both a LiDAR (rightmost, circle points) and an FMCW Radar (rightmost, yellow squares) on a moderately rainy day (test scenario 4 as defined in **Table 4**).

Outcomes revealed that moderate rain exerted little influence on image clarity for both RGB and thermal cameras, enabling straightforward separation of the ISO barrel from background elements (leftmost and second from left positions in **Figure 12**). In the thermal image, a mirrored reflection of the ISO barrel created by water on the ground held potential to trigger mistaken judgments within the perception system.

The stereo camera captured shape-related features of the ISO barrel amid moderate rain (middle position in **Figure 12**). Yet, multiple ground sections remained unregistered. At the same time, numerous airborne 3D points surfaced behind obstacles, thereby diminishing detection confidence.

The ToF camera failed to register either the ISO barrel or ground surfaces because insufficient active light reached the sensor under rainy conditions (second from right in **Figure 12**). In addition, various ground portions remained undetected owing to uncertainties in stereo image alignment arising from uniform surface areas. Furthermore, abundant floating 3D point clouds appeared behind obstacles, making detection confidence difficult to assess.

Conversely, LiDAR and FMCW Radar achieved steady detection of the ISO barrel under rainy conditions (rightmost position in **Figure 12**). However, LiDAR overlooked the majority of ground surfaces, as water layers on asphalt absorbed laser signals or acted as mirror-like reflective planes that redirected light in patterns distinct from those in dry states.

Low visibility conditions (test scenarios 4 and 5)

Figures 13 and 14 compare RGB and thermal images with a depth image from the stereo camera in dim and fully dark environments.

© 2025 The Author(s). | Published by Agro Intelligence Research Press



Figure 13. Comparison of an RGB image (left), a thermal image (middle), and a depth image (right) from a stereo camera in low-light conditions.



Figure 14. Comparison of an RGB image (left), a thermal image (middle), and a depth image (right) from a stereo camera in dark conditions.

Under low-light conditions **(Figure 13)**, the RGB camera (left) captured shape features, and the highly reflective road sign remained identifiable even in darkness **(Figure 14, left)**.

The thermal camera identified obstacles independent of light availability (**Figure 13**, middle position), yet distinguishing the road sign from the background proved challenging in darkness (**Figure 14**, middle position) because the obstacle's temperature merged with surrounding temperatures.

The stereo camera was unable to measure objects under both low-light and dark conditions because the stereo matching process could not locate matching feature points across the paired images (**Figures 13 and 14**, right sides).

Evaluation procedure

An evaluation procedure drawn from prior research was applied to assess the suitability of system requirements in an almost objective manner while guiding the selection of appropriate sensors from a sensor database [5]. The three design considerations functioned as primary benchmarks inside this procedure: technical performance, detection reliability, and practical considerations. Careful selection remains necessary for evaluation benchmarks tied to each consideration, while accounting for the overall system concept, environmental settings, stressors, and the boundaries of the planned use. Designers or manufacturers establish evaluation benchmarks on a subjective basis, based on system requirements. For example, technical performance benchmarks could incorporate perception range, range accuracy, refresh rate, and perception density; detection reliability benchmarks could address illumination conditions, precipitation conditions, and object occlusion; practical considerations benchmarks could encompass cost and IP enclosure rating.

© 2025 The Author(s). | Published by Agro Intelligence Research Press

Each benchmark is assigned a minimum threshold and a weight value in the range 0 to 1. Elevated weight values indicate greater significance attached to that particular evaluation benchmark. Minimum thresholds are derived from the technical safety concept and foundational hardware. Assessment of individual perception sensors proceeds by verifying compliance with minimum thresholds and observing sensor capabilities across all evaluation benchmarks. Scoring for each evaluation benchmark is on a 6-point scale, followed by the application of weights, where higher scores indicate greater suitability [5]. Scores are derived from technical specifications and outcomes from actual testing. In conclusion, a normalized evaluation score is computed for each perception sensor by dividing the sum of (weight × score value) by the sum of (weights × peak score value). The resulting normalized evaluation score supports direct numerical comparison against sensors belonging to identical or differing categories.

Results and Discussion

This section provides broad details on the perception sensors, based on hands-on testing. The closing section presents outcomes from the assessment of multiple perception sensors applied to the “autonomous grass mower” scenario, with expanded information provided in the following sections.

Comparison of perception sensors

Table 7 provides a consolidated overview of comparisons and assessments conducted on the studied perception sensors. Drawing from testing outcomes combined with literature analysis, key attributes of the perception sensors include:

Table 7. Summary of comparison and evaluation of investigated perception sensors.

Category	Parameter	RGB camera	Thermal camera	Stereo camera	CW-ToF camera	LiDAR	FMCW r
Technical capabilities	Maximum sensing distance	Approximately 100 m	Approximately 20 m	• o 1.%2	Approximately 4 m	Approximately 100 m	Approxim 80 m
	Frame/refresh rate	Up to 30 fps	Up to 60 fps	Up to 40 fps	• o 1.%2	Up to 45 fps	Up to 20
	Distance measurement precision	—	About 10 cm	About 4 cm	About 3 cm	About 20 cm	—
	Image/data resolution	1920 × 1080 pixels	640 × 512 pixels	1600 × 1200 pixels	224 × 171 pixels	Angular resolution (up to 0.1° × 2°)	Approxim a maximu 250 poi
	Viewing angle	78° × 49°	50° × 41°	61.6° × 48.1°	62° × 45°	360° × 30°	120° ×
	Perception density (PD)	PDH | PDV [points/°]	24.6 | 22.04	12.8 | 12.5	26 | 25	3.6 | 3.8	10 | 0
		PDHV [points/°]	23.3	12.6	25.8	3.6	2.2
	Achievable perception	Recognition	Observation	Recognition	Detection	Monitoring	None

© 2025 The Author(s). | Published by Agro Intelligence Research Press

	detail level [39]						
Operational and environmental factors	Detection reliability	Moderate rain conditions	Highly suitable	Highly suitable	Moderately suitable	Not suitable	Modera suitab
		Low-light conditions	Low suitable	Highly suitable	Not suitable	Highly suitable	Highl suitab
		Dark conditions	Not suitable	Highly suitable	Not suitable	Highly suitable	Highl suitab
		Grass penetration capability	Not suitable	Highly suitable	Not suitable	Not suitable	Not suit
Practical considerations	Processing cost for depth estimation	—	Relatively high	Relatively low	Relatively low	Relatively low	—
	Data bandwidth demand	Relatively high (below 1500 Mbps)	Relatively medium (below 300 Mbps)	Relatively high (below 2450 Mbps)	Relatively medium (below 80 Mbps)	Relatively medium (below 80 Mbps)	Relatively (below Mbps
	Physical size	Relatively compact	Relatively compact	Relatively small to medium	Relatively compact	Relatively medium to large	Relativ compa
	Cost level	Low	Medium	Medium	Medium	High	Mediu

An RGB camera is an economical choice that can record visible signals resembling human visual input. It provides a high perception density, which supports applications in monitoring and object and feature identification. Nevertheless, surrounding illumination states exert substantial effects on its functioning. Powerful direct illumination or insufficient lighting can create visibility challenges. At the same time, accumulations of dust, snow, or similar materials on the lens may distort captured images or narrow the field of view [14]. Attention must focus on these unsafe behaviors to maintain security in automated processes. Application of video compression approaches such as H.264 and M-JPEG within the RGB camera reduces transmitted data volume, though resulting compression distortions may mislead algorithms used in machine vision.

A thermal camera generates images of objects based on heat signatures rather than visible attributes. It offers insufficient perception density for reliable object identification at extended distances compared to the RGB camera [18]. Nevertheless, it performs effectively for monitoring living entities or nighttime observation, regardless of lighting conditions, and can observe through vegetation. The thermal camera produces no visible contrast levels and cannot interpret printed text or graphic elements. Additionally, it cannot penetrate glass, which prevents mounting behind forward-facing windows.

A stereo camera delivers comprehensive field-of-view 3D data collection with high perception density; however, surfaces lacking texture are not estimated, resulting in 3D voids. Functioning is difficult in low-light or dark environments when relying on paired RGB cameras [40]. The stereo matching operation itself is complex and requires significant processing time, necessitating hardware acceleration via a Graphics Processing Unit (GPU) or Field Programmable Gate Array (FPGA).

© 2025 The Author(s). | Published by Agro Intelligence Research Press

A CW-ToF camera determines distances by illuminating objects with brightness-modulated light, yielding better perception density than either LiDAR or FMCW radar during obstacle identification tasks. Nonetheless, challenges arise in bright sunlight or in the presence of powerful near-infrared light. Restricted emitted light strength limits operations to short distances and impairs proper distance calculation when surface reflections are perceived as excessively intense or faint.

LiDAR dispatches hundreds of thousands of beams every second, achieving strong precision over roughly 100 m, yet vertical perception density remains comparatively low relative to camera systems, which complicates object classification. Raindrops can be registered as objects while simultaneously narrowing the effective performance range. The specific LiDAR used in this assessment incorporates mechanical moving components, which increase the risk of breakdown or malfunction and raise maintenance costs.

FMCW radar transmits radio waves that reflect from objects and calculates both relative object speeds and distances directly. This method provides an affordable solution for perception tasks in challenging weather, though angular discretization limitations arising from sensor dimensions and perception density hinder clear differentiation among obstacles. Effects of multipath propagation can be substantial, including signal disruptions, detection inaccuracies, and angular measurement errors.

Evaluation results

Table 8 presents a sample instance of the evaluation procedure, along with the corresponding outcomes, for a stereo camera when applied to the example scenario of an autonomous grass mower equipped with obstacle detection. **Figure 15** depicts the outcomes of the evaluation procedure across several perception sensors in the “autonomous grass mower” scenario. Mean values calculated for technical performance, detection reliability, and practicality facilitate comparisons aligned with system requirements applicable to each perception sensor.

Table 8. An example of evaluating a stereo camera using an evaluation procedure for an autonomous grass mower with obstacle detection is presented. The rating scale is as follows: not suitable (0), very low suitable (0.2), low suitable (0.4), marginally suitable (0.6), moderately suitable (0.8), and highly suitable (1).

Category	Rephrased content
Example application	Autonomous lawn mower equipped with obstacle detection capability
System specifications	• Maximum operating velocity: up to 33 km/h (minimum stopping distance of 8 m required)• Required perception and response time: 100 ms (10 Hz) • Core functions: object detection and distance estimation (accuracy within 10 cm), GNSS-supported localization, object classification (minimum observation level according to IEC 62676), and safe operational control
Environmental conditions	• Lighting conditions: bright sunlight and low-light environments • Weather conditions: moderate rainfall
Hazard source	Physical obstacles (positive objects such as trees, humans, etc.)
System limitations	Inability to reliably detect very small or negative obstacles; degraded performance under severe weather conditions (e.g., intense rain, heavy snowfall, dense fog, etc.)

© 2025 The Author(s). | Published by Agro Intelligence Research Press

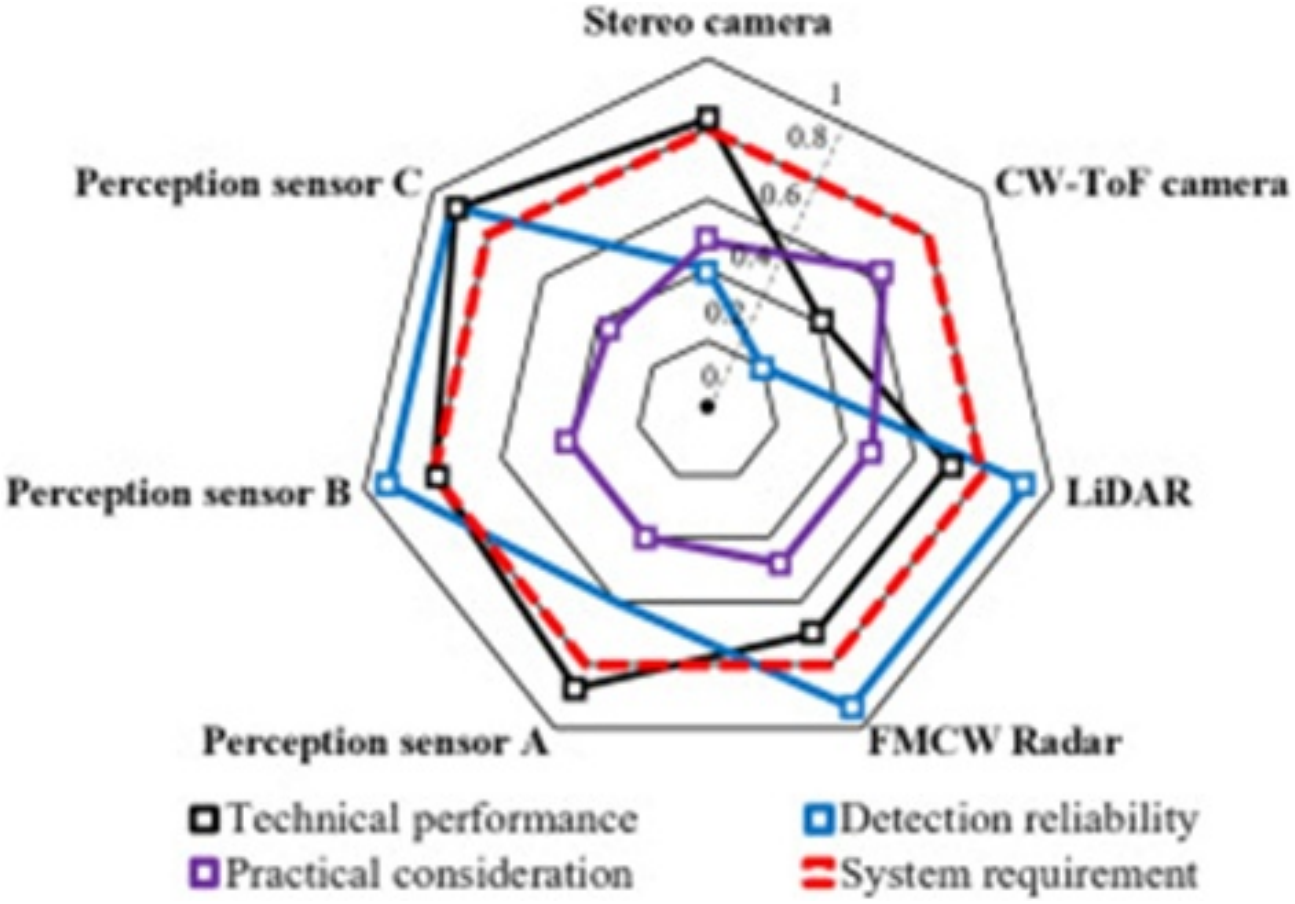

Figure 15. The results of the exemplary evaluation of several perception sensors for an autonomous grass mower with obstacle detection. The evaluation values are normalized. The dashed red line at 0.8 (“moderately suitable”) defines the minimum required system performance level. Perception A, B, and C are placeholders that contain normalized evaluation values for arbitrary sensors from a sensor database.

Conclusion

Regrettably, no single sensor exists that achieves flawless obstacle detection across all operating conditions while meeting the requirements of the specified use case, as demonstrated in **Table 8** and **Figure 15** [33]. Sensors can fail or generate erroneous readings, which diminish machine productivity and operational effectiveness. Overcoming these constraints involves integrating complementary sensor technologies into a unified perception system, as highlighted by the evaluation procedure outcomes in **Table 8** [11]. For instance, LiDAR sensors deliver precise 3D structural data, whereas RGB cameras record dense scene details. Merging such diverse technologies delivers superior results by offsetting individual sensor shortcomings and ensuring reliable identification across diverse settings.

The workflow for creating a functionally safe and dependable perception system is shown in **Figure 16**. Before validating the perception system design, confirming the perception functions is essential to ensure they are appropriate and thorough for the planned application, which is achieved by examining perception sensors or systems per ISO 21448, ISO 25119, and ISO 18497. All faults or operational failures require detection and correction to remove or lessen dangerous actions. Ultimately, the machine manufacturer must pinpoint any shortcomings, restrictions, or opportunities for improvement [3].

© 2025 The Author(s). | Published by Agro Intelligence Research Press

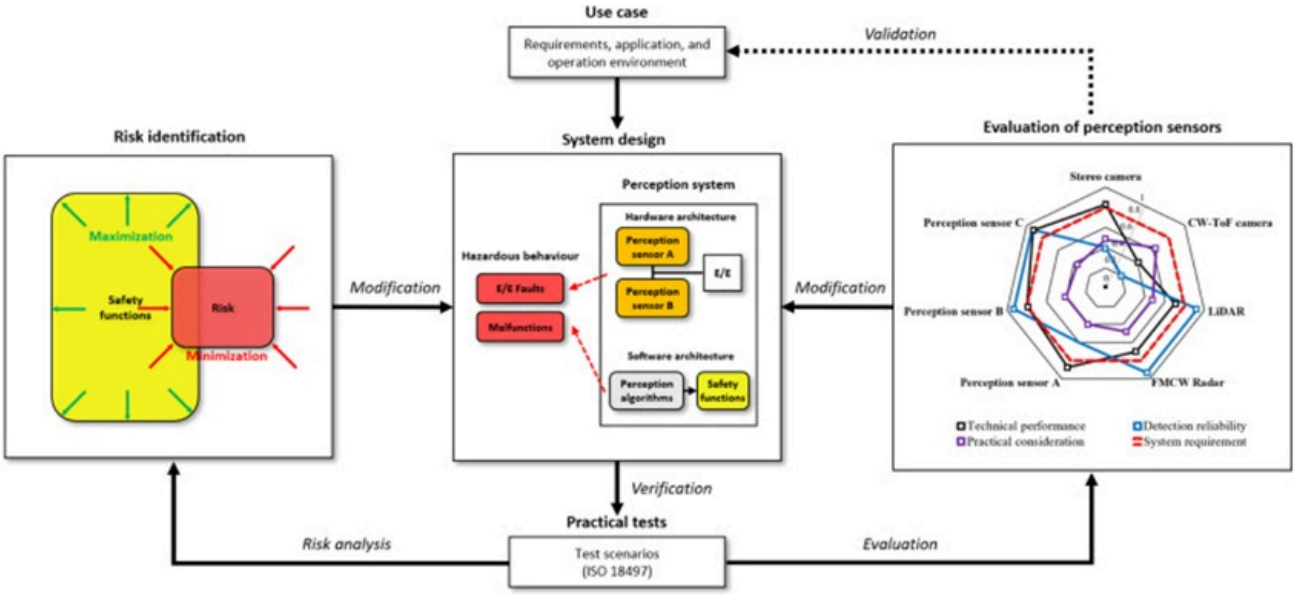

Figure 16. Iteration process for designing a functionally safe and reliable perception system.

This research outlines a broad method for the creation and confirmation of a functionally safe and dependable perception system, drawing on ISO 21448, ISO 25119, and ISO 18497 as guiding references. Three core design aspects were detailed: technical performance, detection reliability, and practical considerations. To confirm performance demands on perception sensors, sample test scenarios were developed to reflect actual working environments, covering obstacles targeted for identification, anticipated visibility issues, testing locations, and varying illumination levels. These test scenarios might serve as a foundation for future assessment standards by other research groups, facilitating consistent outcomes and building a shared community database. Real-world trials were conducted on a test platform to examine perception sensor capabilities for obstacle identification. Field trial outcomes were analyzed and assessed in accordance with the established design aspects, after which sensors received near-numerical scores using the evaluation method from an earlier study [5].

The main takeaways and future directions include the following:

• Design aspects for a perception system derive from a functional safety framework under realistic operating situations. “Technical performance” and “detection reliability” are vital elements in building functionally safe and dependable perception systems across varied environmental settings.

• The five levels of pixel density outlined in IEC 62676 function as benchmarks to categorize the needed detail level for a target under detection at a specified target distance. A novel criterion, termed “perception density,” emerges as a fresh standard for setting technical demands to achieve obstacle detection or classification capabilities. This measure further supports uniform comparisons of spatial resolution across different perception sensor types, including LiDARs and cameras.

• Environmental, obstacle-related, and machine-related parameters form central risk elements impacting detection reliability in perception sensors. Such elements can cause malfunctions in perception sensors, thereby reducing their confidence levels.

• “Practical considerations”, encompassing factors like cost, physical demands, and regulatory needs, play a critical role during the creation and implementation of a perception system. The specific elements requiring attention will vary depending on the particular system application.

© 2025 The Author(s). | Published by Agro Intelligence Research Press

• The sample test approach offers one streamlined way to confirm minimum performance demands for perception sensors focused on obstacle detection. Nonetheless, addressing real operating situations requires additional confirmation tests or techniques, for example, at the HAAM's peak operating speed, through simulations, or via monitoring during active use.

• The evaluation procedure offers a broad method for supplying safety demands, verification approaches, and application-linked aspects to secure a proper safety level within a perception system.

• Assessment of every sensor covers technical performance, detection reliability, and practical considerations. Consistent with the needs of a particular use case, perception sensors of matching or varying types undergo near-numerical comparisons, guiding system engineers in choosing suitable sensors or sensor groupings to meet their purposes.

• Analysis and testing of perception sensors must uncover potential risks along with any shortcomings, restrictions, or enhancement areas to remove or lessen dangerous actions per ISO 21448, ISO 25119, and ISO 18497.

• Failures within a perception system or its sensors can introduce hazards to highly automated machines. Subsequent efforts will focus on developing a fault management system capable of identifying and assessing dangerous actions within a perception system.

Acknowledgements

None

Conflict of interest

None

Financial support

None

Ethics statement

None

Received: 12 Aug 2023 Revised: 17 Oct 2023 Accepted: 03 Nov 2023
Published online: 25 May 2025

Rights and permissions

Open Access The author(s) retain copyright. This article is licensed under the Creative Commons Attribution-NonCommercial-ShareAlike 4.0 International License. It may be shared and adapted for non-commercial purposes with appropriate attribution, an indication of changes, and distribution of adaptations under the same license. Third-party material may be subject to separate terms identified in its credit line. View the license at https://creativecommons.org/licenses/by-nc-sa/4.0/.

References

1. Edan Y, Han S, Kondo N. Automation in agriculture. In: Springer handbook of automation. Berlin Heidelberg: Springer; 2009. p. 1095-128.
https://doi.org/10.1007/978-3-540-78831-7_63.

2. Linenko AV, Gabitov II, Siraev SF, Aznagulov AI, Lukyanov VV, Kamalov TI. Farm tractor mechatronic steering module. J Appl Eng Sci. 2019;17.
https://doi.org/10.5937/jaes17-22052.

3. ISO. Safety of highly automated agricultural machines – principles for design. First edition. Geneva: International Organization for Standardization; 2018. p. 18497.

4. Zhang Q. Precision agriculture technology for crop farming. Boca Raton: Taylor and Francis; 2016.
https://doi.org/10.1201/b19336.

5. Lee C, Schaetzle S, Lang SA. Evaluation of perception sensors for safety of highly automated machine operations. Proceedings of the LAND.TECHNIK 2022. 2022:163-70.
https://doi.org/10.51202/9783181023952-163.

6. Christiansen P. TractorEYE: vision-based real-time detection for autonomous vehicles in agriculture. PhD dissertation. Department of Engineering, Aarhus University; 2017.
https://doi.org/10.7146/aul.277.192.

7. Moorehead SJ, Wellington CK, Gilmore BJ, Vallespi C. Automating orchards: A system of autonomous tractors for orchard maintenance. Proceedings of the IEEE International Conference on Intelligent Robots and Systems (IROS), Workshop on Agricultural Robotics. 2012.

8. Blume T, Stasewitsch I, Schattenberg J, Frerichs L. Objekterkennung und Positionsbestimmung in der Landwirtschaft am Beispiel eines Ankoppelassistenten. Landtechnik. 2018;73:1-9.
https://doi.org/10.15150/lt.2018.3176.

9. Portugal D, Cabrita G, Gouveia BD, Santos DC, Prado JA. An autonomous all terrain robotic system for field demining missions. Robot Auton Syst. 2015;70:126-44.
https://doi.org/10.1016/j.robot.2015.02.013.

10. Demaitre E. John Deere unveils fully autonomous tractor at CES 2022. Robotics 24/7. 2022.
https://www.robotics247.com/article/john_deere_unveils_fully_autonomous_tractor_ces_2022

11. ISO. Safety-related parts of control systems. Second edition. Geneva: International Organization for Standardization; 2018. p. 25119.

12. ISO. Safety of the intended functionality. ISO 21448. Geneva: International Organization for Standardization; 2022.

13. Martí E, de Miguel MA, García F, Pérez J. A review of sensor technologies for perception in automated driving. IEEE Intell Transp Syst Mag. 2019;11(4):94-108.
https://doi.org/10.1109/MITS.2019.2907630.

14. Szeliski R. Computer vision: algorithms and applications. New York: Springer Science & Business Media; 2010.

15. Jiang P, Ergu D, Liu F, Cai Y, Ma B. A review of YOLO algorithm developments. Procedia Comput Sci. 2022;199:1066-73.
https://doi.org/10.1016/j.procs.2022.01.135.

16. Jung T-H, Cates B, Choi I-K, Lee S-H, Choi J-M. Multi-camera-based person recognition system for autonomous tractors. Designs. 2020;4:54.

© 2025 The Author(s). | Published by Agro Intelligence Research Press

https://doi.org/10.3390/designs4040054.

17. Panda SK, Lee Y, Jawed MK. Agronav: autonomous navigation framework for agricultural robots and vehicles using semantic segmentation and semantic line detection. Proceedings of the IEEE/CVF Conference on Computer Vision and Pattern Recognition (CVPR). 2023. p. 6271-80.

18. Nilsson F. Intelligent network video: Understanding modern video surveillance systems. First edition. Boca Raton: Taylor and Francis; 2008.

19. Christiansen P, Steen KA, Jørgensen RN, Karstoft H. Automated detection and recognition of wildlife using thermal cameras. Sensors. 2014;14:13778-93.
https://doi.org/10.3390/s140813778.

20. Steen KA, Villa-Henriksen A, Therkildsen OR, Green O. Automatic detection of animals in mowing operations using thermal cameras. Sensors. 2012;12:7587-97.
https://doi.org/10.3390/s120607587.

21. Sebe N, Lew MS. Robust computer vision: theory and applications. Dordrecht: Springer Science and Business Media; 2013.

22. Fue K, Porter W, Barnes E, Li C, Rains G. Evaluation of a stereo vision system for cotton row detection and boll location estimation in direct sunlight. Agronomy. 2020;10:1137.
https://doi.org/10.3390/agronomy10081137.

23. Zhang S, Wang Y, Zhu Z, Li Z, Du Y, Mao E. Tractor path tracking control based on binocular vision. Inf Process Agric. 2018;5:422-32.
https://doi.org/10.1016/j.inpa.2018.07.003.

24. Hansard M, Lee S, Choi O, Horaud RP. Time-of-flight cameras: principles, methods and applications. New York: Springer Science and Business Media; 2012.

25. Gai J, Xiang L, Tang L. Using a depth camera for crop row detection and mapping for under-canopy navigation of agricultural robotic vehicle. Comput Electron Agric. 2021;188:106301.
https://doi.org/10.1016/j.compag.2021.106301.

26. Fu L, Gao F, Wu J, Li R, Karkee M, Zhang Q. Application of consumer RGB-D cameras for fruit detection and localization in field: a critical review. Comput Electron Agric. 2020;177:105687.
https://doi.org/10.1016/j.compag.2020.105687.

27. Avadhanulu M. An introduction to lasers: theory and applications. New Delhi: S. Chand Publishing; 2001.

28. Debnath S, Paul M, Debnath T. Applications of LiDAR in agriculture and future research directions. J Imaging. 2023;9:57.
https://doi.org/10.3390/jimaging9030057.

29. Andújar D, Escolà A, Rosell-Polo JR, Fernández-Quintanilla C, Dorado J. Potential of a terrestrial LiDAR-based system to characterise weed vegetation in maize crops. Comput Electron Agric. 2013;92:11-5.
https://doi.org/10.1016/j.compag.2012.12.012.

30. Kissinger D. Millimeter-wave receiver concepts for 77 GHz automotive radar in silicon-germanium technology. New York: Springer Science and Business Media; 2012.

31. Rouveure R, Nielsen M, Petersen A, Reina G, Foglia M, Worst R, et al. The QUAD-AV Project: multi-sensory approach for obstacle detection in agricultural autonomous robotics. Proceedings of the International Conference of Agricultural Engineering (CIGR-Ageng). 2012. p. 8-12.

© 2025 The Author(s). | Published by Agro Intelligence Research Press

32. Santos PH, Gimenez LM, Maldaner LF, da Costa Duarte C. Performance analysis of a RADAR FMCW sensor developed for plant height measurement in agriculture and comparison with an NDVI sensor. Proceedings of the GEOINFO. 2019. p. 147-57.

33. ISO. Object detection systems and visibility aids performance requirements and test. ISO; 2017. p. 16001.

34. European Union. Vehicle braking requirements for the approval of agricultural and forestry vehicles. EC - European Union; 2015. p. 139.

35. Brahmi M, Siedersberger K-H, Siegel A, Maurer M. Reference systems for environmental perception: requirements, validation and metric-based evaluation. Proceedings of the 6th Tagung Fahrerassistenzsysteme. 2013.

36. Rehrl K, Gröchenig S. Evaluating localization accuracy of automated driving systems. Sensors. 2021;21:5855. https://doi.org/10.3390/s21175855.

37. Li Y, Chen Y. Driver vision based perception-response time prediction and assistance model on mountain highway curve. Int J Environ Res Public Health. 2017;14:31. https://doi.org/10.3390/ijerph14010031.

38. Berk M. Safety assessment of environment perception in automated driving vehicles. Technische Universität München; 2019.

39. IEC. Video surveillance systems for use in security applications. IEC 62676. Geneva: International Electrotechnical Commission; 2014. p. 143.

40. Sanchez-Rodriguez J-P, Aceves-Lopez A. A survey on stereo vision-based autonomous navigation for multi-rotor MUAVs. Robotica. 2018;36:1225-43. https://doi.org/10.1017/S0263574718000358.

© 2025 The Author(s). | Published by Agro Intelligence Research Press